Landslides (2018) 15:879-893 DOI 10.1007/s10346-017-0898-4 Received: 23 February 2017 Accepted: 17 September 2017 Published online: 15 November 2017 © Springer-Verlag GmbH Germany 2017 Dunlong Liu · Xiaopeng Leng · Fanggiang Wei · Shaojie Zhang · Yong Hong

Visualized localization and tracking of debris flow movement based on infrasound monitoring

Abstract During the initiation and movement of debris flow, low frequency infrasound is generated and emitted with characteristics such as strong penetration, low attenuation, and a high propagation speed that is faster than the debris flow. Monitoring infrasound has been used in debris flow detection and early warning systems; however, although the current infrasound-based warning system of debris flow can provide an alarm when debris flow occurs, it cannot locate and track the movement of debris flow in real time, and cannot determine the arrival time of debris flow to its potential victims. Thus, the potential applications of low frequency infrasound in debris flow disaster prevention and reduction have not yet been fully explored. In this study, we constructed an optimal triangular monitoring array based on factors such as the terrain of the monitoring area and characteristics of infrasound propagation. Combined with the timedelay estimation method, we determined and established an acoustic source localization model based on the time difference of arrival. Furthermore, with the help of a GIS platform, a visualized localization and tracking system for debris flow movement was developed to achieve real-time monitoring of debris flow. The performance of the system on acoustic source localization was validated using a simulation test and long-term field monitoring of debris flow at Jiangjia gully in Dongchuan, Yunnan province, China. Both the simulation and field test results showed that the system has high localization accuracy and strong real-time response. The results of the monitoring system could provide more accurate warning information of debris flow to local government and residents, allowing them to take appropriate mitigation measures well in advance to reduce the loss of life and property caused by debris flows.

Keywords Debris flow · Infrasound · Monitoring · Visualized localization

Introduction

Debris flow infrasonic signals are those originated from rock breaking, collisions, and frictions between the flow surge front and the channel bed and bank slopes during the debris flow formation and movement (Chou et al. 2013). Compared to the speed of debris flows (generally 5-20 m/s, Kang 1993), infrasonic waves may propagate dozens of times faster, being characteristically of low attenuation, strong penetrability, and far reaching (Lin and Yang 2010; Xu et al. 2013). Therefore, the monitoring of debris flow infrasonic signals can advance the information availability regarding debris flow occurrences for issuing hazard-disaster warnings (Zhang and Yu 2010; Zhong et al. 2011).

Infrasound monitoring in early warning of debris flow has been widely acknowledged in recent years. Many scholars are actively carrying out extensive research and exploration on this topic. Zhang et al. (2004) observed and analyzed infrasound signals from debris flow in Jiangjia gully, Yunnan province, China, and concluded that the dominant frequency of infrasound from viscous debris flow is between 5 and 10 Hz. Chou et al. (2007, 2013) observed and analyzed infrasound signals from debris flow in Huoyan Mountain, Taiwan,

and indicated that the dominant frequency range of infrasound from dilute debris flow (5-15 Hz) is wider than that from viscous debris. In addition, Chou et al. (2007, 2013) suggested the interference by environmental noise such as wind and rain should be considered in practice. Hübl et al. (2008) carried out experiments to monitor the infrasound from debris flow in Jiangjia gully and suggested that the peak of infrasound from debris flow lies between 8 and 12 Hz and the sound pressure is usually less than 4 Pa. Zhang and Yu (2008, 2010) developed an infrasound monitoring device for debris flow observation and an early warning system of debris flow by integrating rain gauge and image transmission equipment. Kogelnig et al. (2011, 2014) conducted infrasound monitoring experiments for debris flow in different watersheds and indicated that the monitoring of infrasound produced by debris flow has great potential. Li et al. (2012) developed an infrasound monitor for debris flow to monitor the debris flow gullies alongside a railroad. However, these systems have two problems in terms of their practical application: first, the monitoring does not rule out the interference from environmental noise (such as wind, lightning, and blasting), and often produces false alarms; and second, it is unable to determine the real-time position of debris flow during its movement, thus failing to determine the length of time until the debris flow would reach its victims and failing to reach its full potential in disaster reduction.

For the first problem, by distinguishing the key characteristic parameters of infrasound from debris flow and environmental interference, Liu et al. (2015) presented a new method for the recognition of the infrasonic signal to solve the problem of frequent false alarms and substantially increase the accuracy of early warning. To our knowledge, there has not yet been any research focusing on the aforementioned second problem. Nonetheless, in recent years, acoustic source localization technique based on infrasound monitoring arrays has been increasingly used in the study of natural disasters (e.g., earthquake and volcanic activity). Extensive studies of observation and localization of the hypocenter have been carried out by analyzing earthquake infrasound from the deployed monitoring arrays (Cansi 1995; Jiang 2002; Pichon et al. 2005; Murayama et al. 2006; Lv et al. 2012; Zhang et al. 2013). In addition, some scholars have also conducted the studies of localization and tracking of volcanic activity and pyroclastic flow with the time-delay estimation method based on monitoring arrays (Matoza et al. 2007, 2009; Ripepe et al. 2010). The Institute of Acoustics, Chinese Academy of Sciences has conducted a considerable amount of research on acoustic source localization technology (Men et al. 2011; Wei et al. 2011; Lu and Yang 2012). These studies provide a reference for use in the real-time location and tracking of movement of debris flow based on infrasound monitoring.

In this study, on the basis of existing research results, an infrasound array was deployed in Jiangjia gully, and infrasonic signals of debris flow were recognized following the infrasound recognition system developed by Liu et al. (2015). Based on the geometric structure of the array and cross-correlated delay estimation method, we developed the acoustic source localization model based on time difference of arrival to achieve the localization of debris flow surges. This

localization model allows the position of debris flow to be located at different time periods. Combined with a GIS platform, this method can provide visualized localization and tracking of debris flow, thus providing more effective infrasound monitoring of debris flow.

Debris flow infrasound and monitoring array

Characteristics of infrasound produced by debris flow

Debris flow is a solid-liquid two phase flow in viscous laminar or diluted turbulent state that contains solid materials such as soil and fragmented rock (Zhang et al. 2009; Liu 2015; Ma et al. 2016). Ranging between hyperconcentrated flow and block movement, the fluid can generate infrasound when flowing rapidly in valleys and gullies. Infrasound generated by debris flow is a spherical wave, propagating in all directions through air. Various environmental factors such as wind, temperature, and atmospheric absorption can interfere with monitoring processes.

(1) Effect of wind on infrasound generated by debris flow

Infrasound generated by debris flow is affected by surface wind when propagating near the ground. When wind passes through buildings, forests, and mountains, it is usually accompanied by pressure fluctuations, which can cause a dramatic pressure change. The pressure change can be expressed by the Bernoulli equation:

$$P + (1/2) \rho V^2 = \alpha \tag{1}$$

where P, ρ , and V are pressure, air density, and wind velocity, respectively, and α is a constant.

Taking derivative with respect to wind velocity V gives:

$$\Delta P = \rho V \Delta V \tag{2}$$

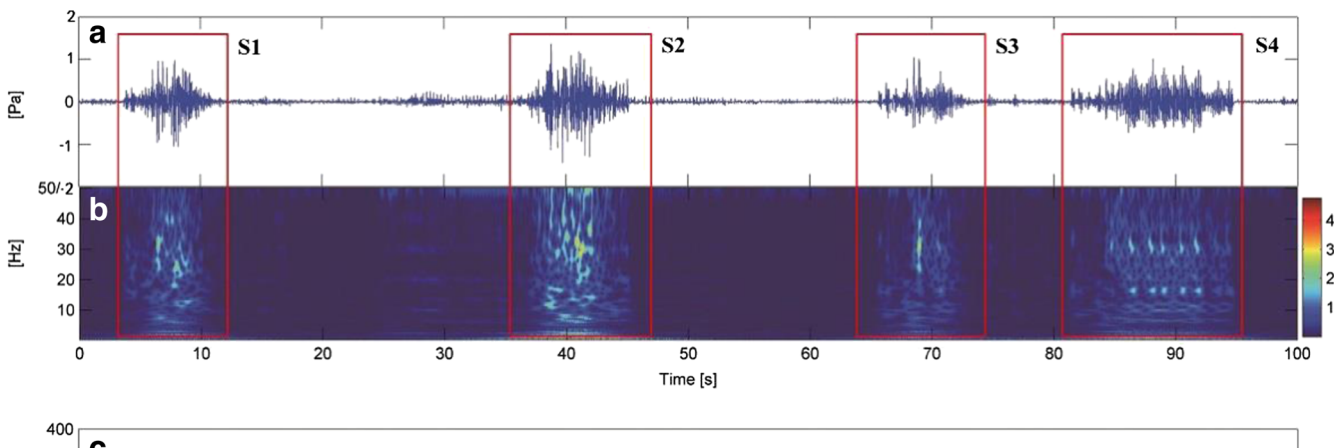
For a wind velocity range of 6.7-11.2 m/s, a pressure change of about 50 Pa is produced, much larger than the infrasound pressure in nature (0.01-5 Pa). It is therefore clear that wind can strongly interfere with infrasound monitoring. Therefore, during the infrasound monitoring, the wind interference needs to be recognized and reduced according to its characteristics.

(2) Effect of temperature on infrasound of debris flow

Studies have shown that the square of sound speed when sound is traveling in air in subaudible region is proportional to the value calculated by dividing elastic adiabatic modulus by density (Remillieux et al. 2012; Groot-Hedlin and Hedlin 2014), i.e.,

$$C^2 = rP/\rho \tag{3}$$

where C is infrasound velocity (m/s), r is a constant (for adiabatic gas, r = 1.402), P is gas pressure (Pa), rP is the elastic adiabatic modulus of atmosphere, and ρ is the air density (kg/m³).



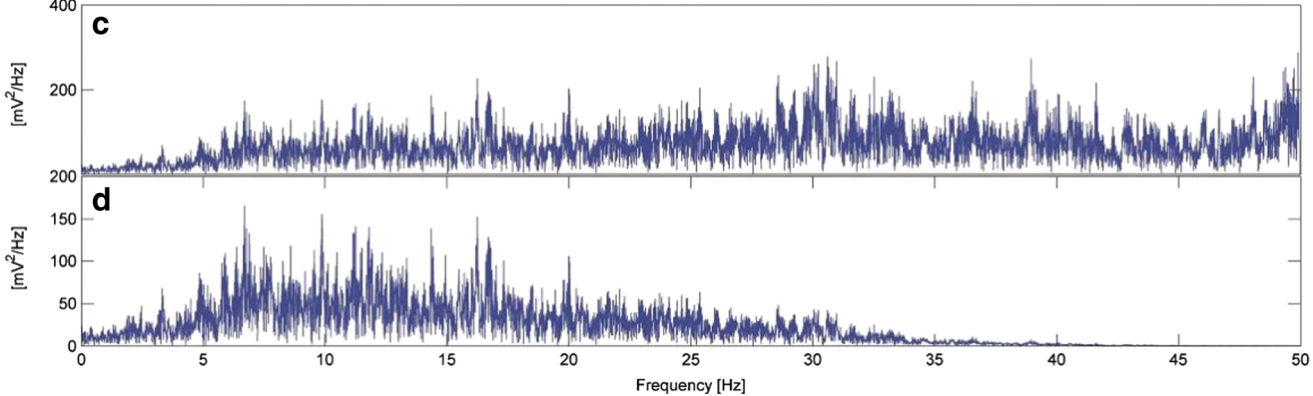


Fig. 1 Sound signals generated from simulated debris flows, a Time series of original signals. b Time-frequency spectrum of original signals. c Power spectra of original signals. d Power spectra of signals through low-pass filtering

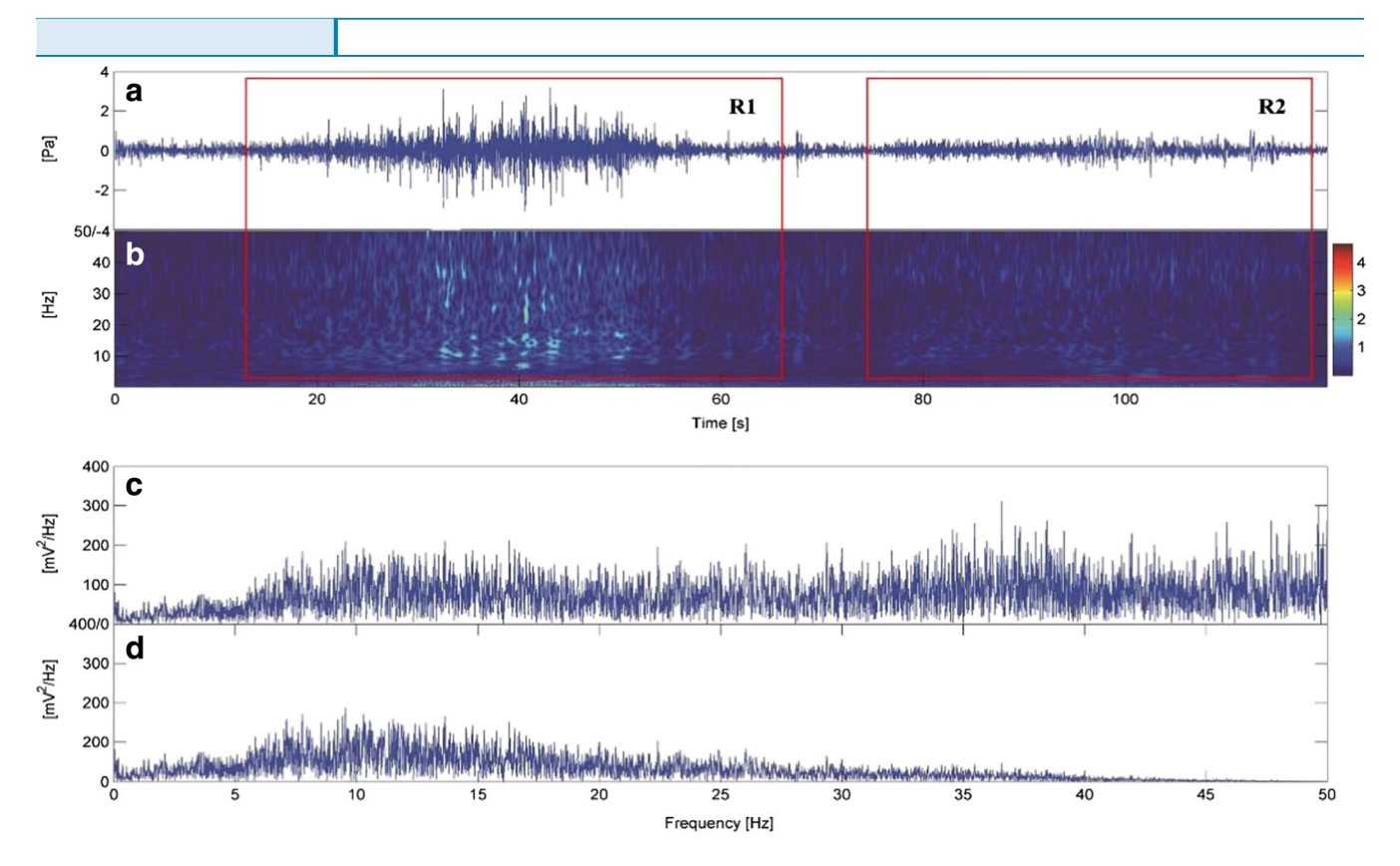


Fig. 2 Sound signals generated from a real debris flow event. a Time series of original signals. b Time-frequency spectrum of original signals. c Power spectra of original signals. d Power spectra of signals through low-pass filtering

The state equation of ideal gas is $P = \rho RT$, where T is the absolute temperature and R is a constant (about 14.33). Substitution of the state equation of ideal gas into Eq. (3) gives

$$C = 20.1\sqrt{T} \tag{4}$$

As indicated by Eq. (4), the propagation velocity of infrasonic wave is only related to temperature and is unrelated to air density and pressure. When temperature is 20 °C, or T = 293 K, C is calculated as 344 m/s. Therefore, the propagation velocity of subaudible sound is comparable with that of audible sound.

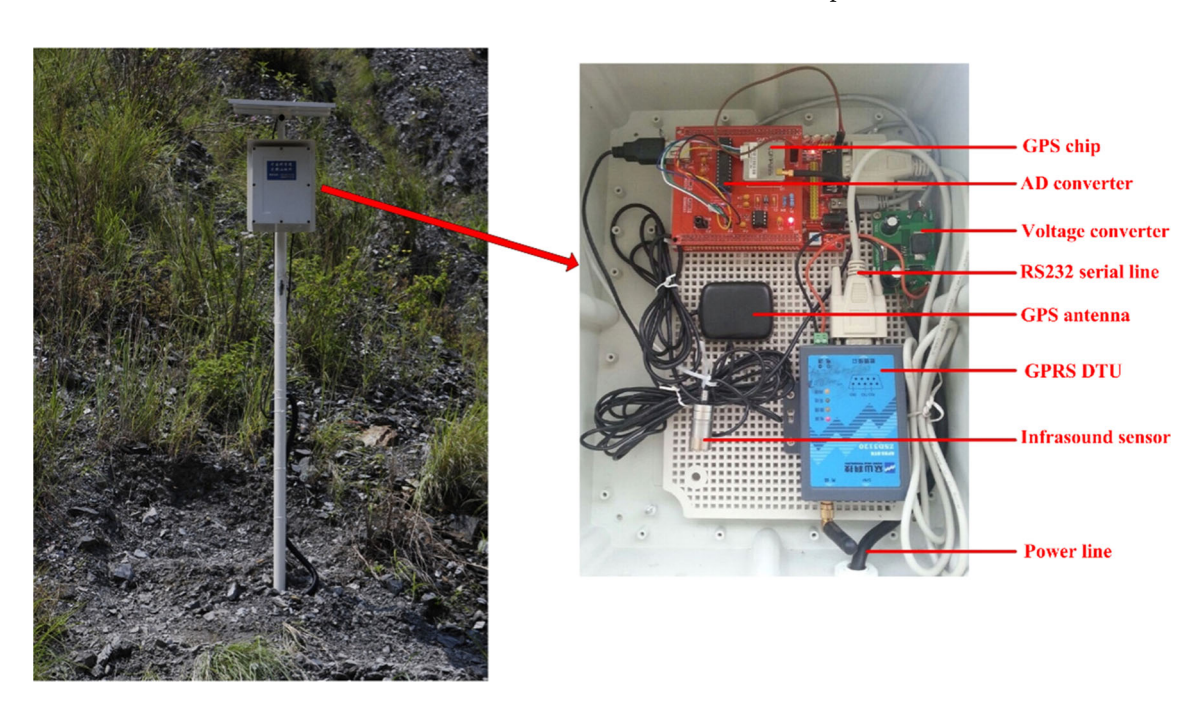


Fig. 3 Collecting and transmitting system for debris flow infrasonic signals

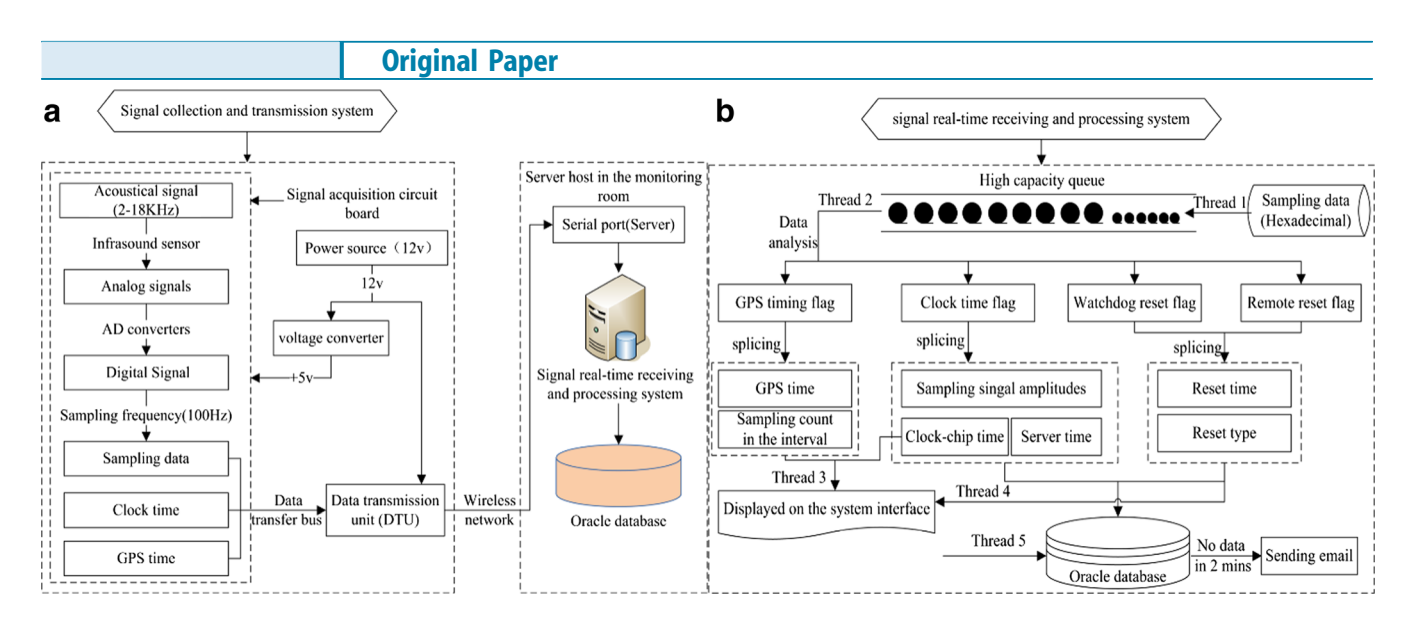


Fig. 4 Working process of the monitoring system for debris flow infrasonic signals. a Working process of the signal collecting and transmitting subsystem. b Working process of the signal real-time receiving and processing subsystem

(3) Energy attenuation of infrasonic waves generated by debris flow

Infrasonic waves propagate in air in the form of energy. The energy attenuates during the propagation process, mainly due to absorption by the atmosphere (such as molecular diffusion, heat transfer, and the viscous effect) (Bass et al. 1972; Pilger and Bittner 2009; Liu 2013). The energy attenuation equation of infrasonic waves caused by atmosphere absorption (Cook 1962; Johnson 2003) is as follows:

$$\begin{cases}
P = P_0 e^{-(\alpha r)} \\
\alpha = 1.6 \times 10^{-4} f^2 / B
\end{cases}$$
(5)

where P indicates the energy of the infrasonic wave received by sensor, P_0 represents the energy of the wave source position, r is the distance between sensor and infrasonic wave (m), α is the absorption coefficient (dB/m), f is the infrasound frequency (Hz), and B is the atmospheric pressure (dyn/cm²).

Equation (5) indicates that the lower the frequency of sound wave, the less the absorption by the atmosphere. The infrasonic wave generated by debris flow propagates near the ground; thus, the maximum absorption coefficient of the infrasonic wave by atmosphere is around 2.0 × 10⁻⁵ dB/km (taking infrasound frequency as 10 Hz and atmosphere pressure near ground as 105 Pa). It is equivalent to 1% energy loss of infrasonic wave after propagation over 5.0×10^4 km. This result shows that the infrasonic wave has little energy attenuation in long-distance propagation. In addition, the frequency of infrasound is low, possessing strong penetration and making it highly suitable for long-distance monitoring.

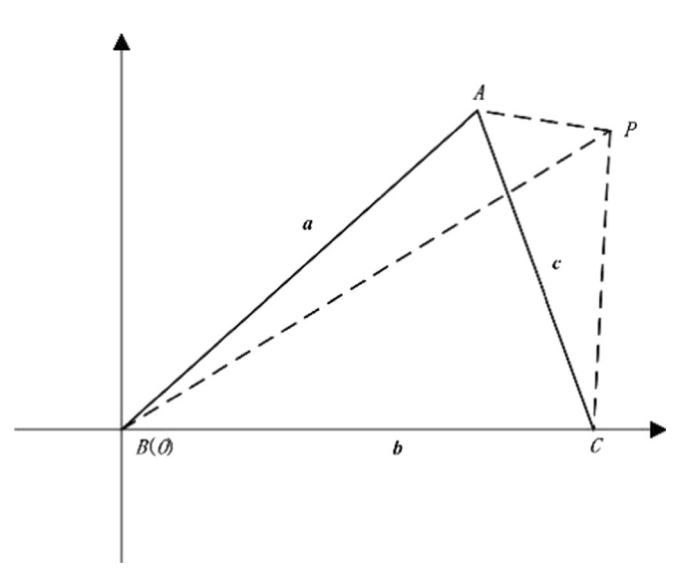


Fig. 5 Translational transformed monitoring array of debris flow infrasound



Fig. 6 Locations of monitoring devices and drumming

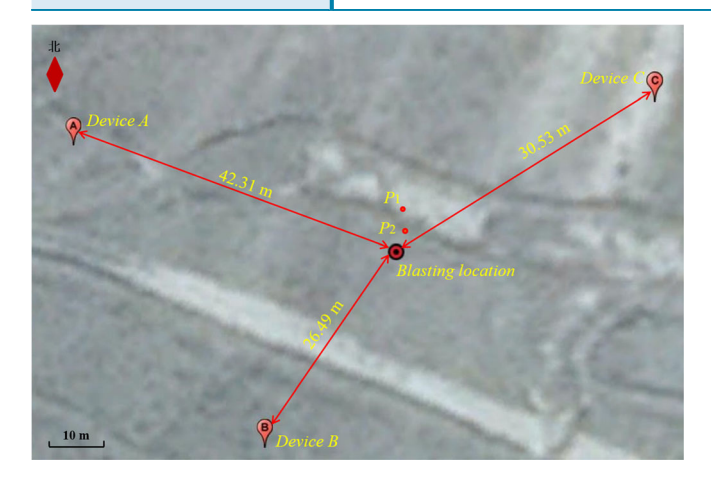


Fig. 7 Locations of monitoring devices and blasting

Infrasound from debris flow is generated on the ground surface and is received by ground-based monitoring stations. Because the infrasound wave propagates near the ground, wind field and temperature field have a little impact on its propagation. Based on the existing studies on infrasound from debris flow and combining large amount of analysis on measured signals (Figs. 1 and 2), the sound pressure of infrasonic wave produced by debris flow was determined to be less than 5 Pa, with a dominant frequency of 5-20 Hz. The waveform of the infrasonic signal shows no clear abrupt change, with a shortterm zero-crossing rate of 0.23-0.32. Compared with other infrasound generated in nature, such as earthquake, lightning, and blasting, infrasound generated by debris flow usually has a longer duration (taking Jiangjia gully as an example, the main gully has a length of 13.9 km, and the speed of debris flow is 5-15 m/s; thus, the time for movement is at least 16 min). Moreover, debris flow is usually composed of several surges. These detailed characteristics of infrasound generated by debris flow provide a more reliable basis to differentiate infrasound generated by debris flow from other infrasound.

Monitoring system of debris flow infrasonic signals

According to the characteristics of debris flow infrasonic signals, we developed a monitoring system for debris flow infrasonic signals by combining SCM (single chip microcomputer) and upper computer. The monitoring system consists of two independent subsystems, namely the collecting and transmitting subsystem and the real-time receiving and processing subsystem. The former (serve as terminal device deployed in debris-flow-prone areas) (Fig. 3) is built on five modules, i.e., high-performance signal acquisition circuit board (STM32 microprocessor, 16-bit bipolar AD converter, and clock chip, working voltage 5v), capacitive infrasound sensor (developed by Institute of Acoustics, Chinese Academy of Sciences), GPS chip, data transmission unit (DTU, working voltage 12v), and power supply unit (Solar panel, 12v leadacid battery, voltage converter, and solar controller). Two types of reset mode (watchdog reset and remote reset) was developed in the system to prevent sampling error of the circuit board for its sudden failures. The latter (running on sever terminal) receives and processes the data remotely transmitted to the server through the virtual serial port (COM port) in real time, which is prepared specifically for the former subsystem deployed in the wild. This subsystem was developed based on the combination of a high capacity queue and five threads concurrent processing, which can realize the functions of display and storage of the sampling data and current status information and prevent data missing for data congestion on server.

High frequency (100 Hz) sampling is proceeded by the signal collecting and transmitting subsystem for debris flow infrasonic signals; clock chip sends out the timestamp information every 10 s (current time of the chip, accurate to the second). The real-time receiving and processing system of debris flow infrasonic signals loads the sampling data into database when parsing out the timestamp logo. Each record in the database contains 1000 sampling points. GPS provides time service to the clock chip every 2 h to synchronize the clock chip time with the satellite time and to ensure that the sampling data have precise time. The signal acquisition circuit board first transmits sampling data to DTU through RS232 serial line, and then DTU transmits the data to the server via

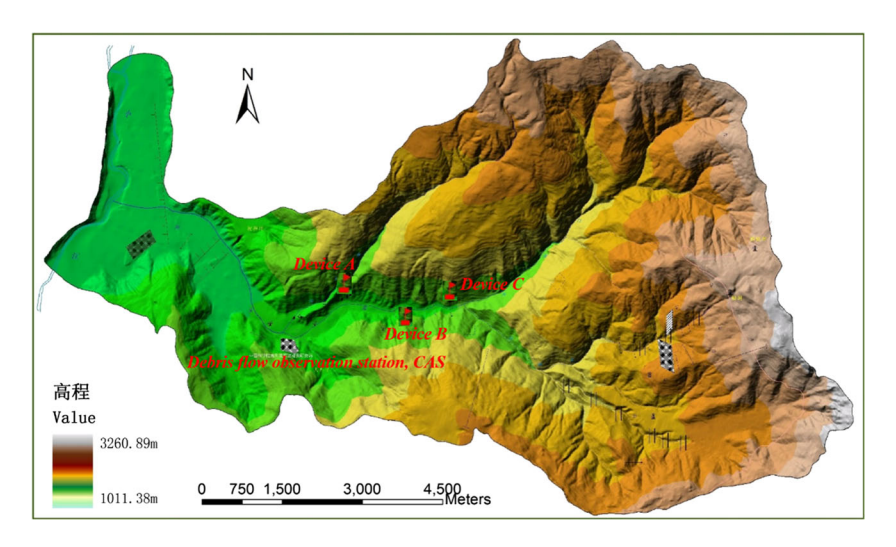


Fig. 8 Monitoring array for debris flow infrasound

wireless network. The working process of the signal collecting and transmitting subsystem and the signal real-time receiving and processing system are shown in Fig. 4a, b, respectively.

Deployment of infrasound monitoring array

The current infrasound monitoring technique uses a single device and does not form a monitoring network. It cannot determine the real-time position of debris flow and its arrival time to victims, limiting its potential for disaster reduction. To achieve more efficient debris flow monitoring, multiple infrasound sensors need to be deployed as an array to locate and track debris flow in real time.

When infrasound generated by debris flow passes through the array, there is a strong correlation between signals received by the distributed array elements. Compared with infrasound signals from debris flow, the disturbance caused by wind and local environment belongs to noise, which shows no or little correlation when received by different elements and can be excluded by correlation analysis. In addition, the different distance between debris flow surge and different elements causes variation in the arrival time of infrasonic signal to different elements, creating a time difference. Therefore, using a sensor array with more than three elements to monitor infrasound generated by debris flow cannot only improve the accuracy of monitoring, but also estimate the location of debris flow based on the arrival time difference of infrasonic signal to different elements, and further locate and track the movement of debris flow in real time.

Different array structures, element numbers, and distances between elements have different impacts on the accuracy of the acoustic source location. In theory, using more elements, a greater distance between the elements (within the monitoring range of the elements), and a more complex array structure can achieve higher accuracy of localization, but the cost of array deployment and data analysis is also higher. Therefore, an appropriate element number, element distance (greater than half of the wavelength of the monitoring signals), and topological structure need to be chosen according to the actual needs of monitoring to achieve optimal localization and tracking. In this study, three sensor devices were chosen to deploy an appropriate monitoring array based on the topography of monitored region, distribution of noise from environmental background (human activity and wind), GPRS network strength, and the propagation characteristics of infrasound generated by debris flow.

Real-time localization and tracking of debris flow surge

Determination of the time-delay estimation method

The time delay refers to the time difference for the same signal to arrive at different elements of a monitoring array. The difference in distance between the wave-surface and the two elements is defined as acoustic path difference (speed of sound multiplied by the time delay). The acoustic source localization method based on time difference of arrival estimates the location of the acoustic source according to the position of each element in an array (element number \geq 3) and the time delay for the same signal to arrive at the different elements. It has wide practical applications

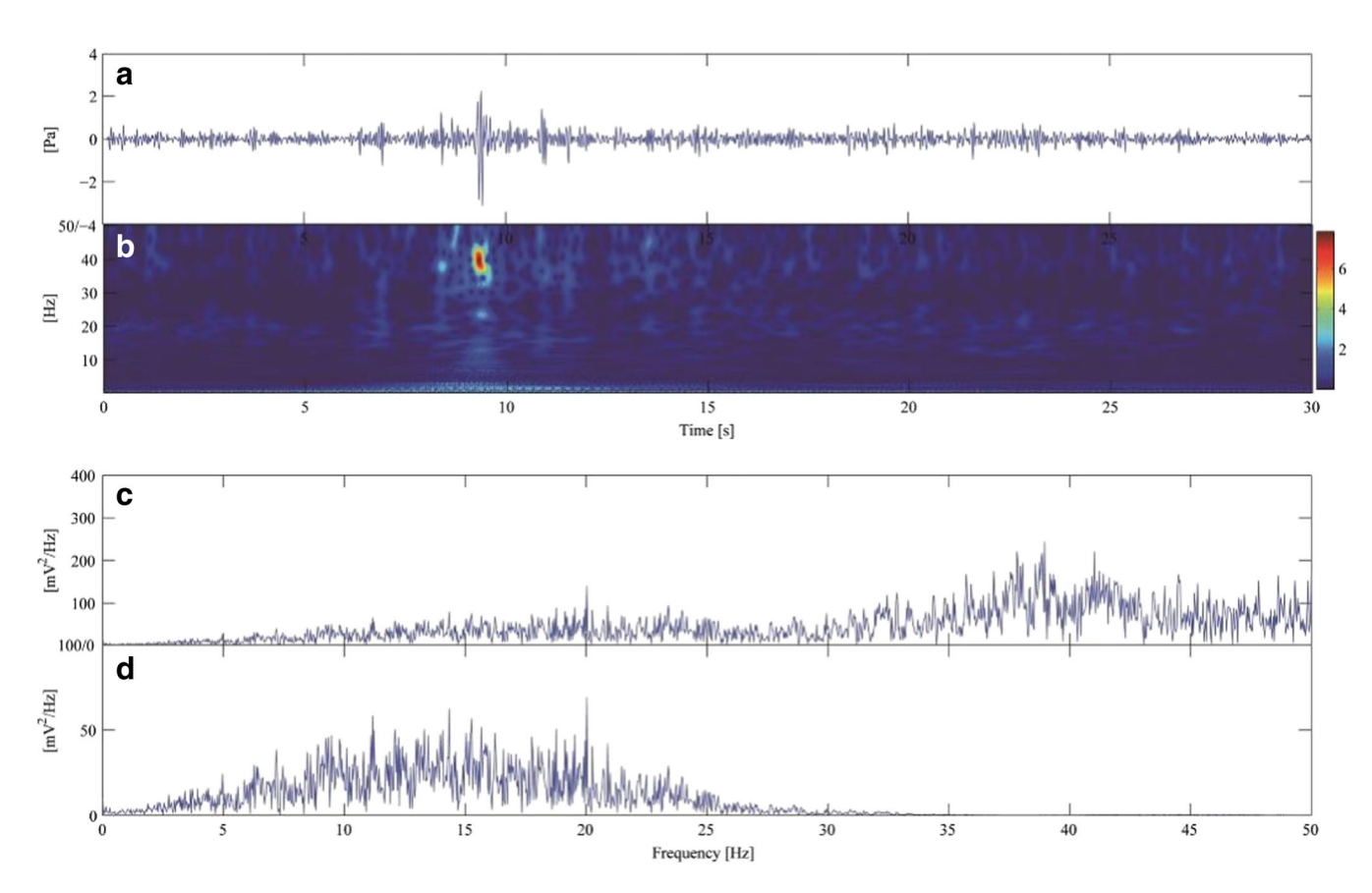


Fig. 9 A section of debris flow infrasonic signals received by device B during event 1. a Time series of original signals. b Time frequency spectrum of original signals. c Power spectra of original signals. d Power spectra of signals through low-pass filtered signals

because of characteristics such as the low computational requirements, ease of implementation, high accuracy of localization, and strong real-time capability (Zhang et al., 2015).

Estimation of the time delay is a critical step in localization based on the time difference of arrival method (Li and Wu 1998; Wang et al. 2000; Yang et al., 2003). The higher the accuracy of the time-delay estimation, the better the localization effect. We selected the generalized cross-correlation (GCC) method in this study because it has high accuracy in time-delay estimation, low computational requirements, and a strong realtime capability. Based on cross-correlated functions, the GCC method weights the power spectrum of signals in the frequency domain and highlights the target signal component, while minimizing the noise component to highlight the peak value of cross-correlated functions at the position of the time delay. The basic principle of the GCC method is to use Fourier transform to transform two signal sequences from the time domain to the frequency domain, calculate their cross-power spectrum, give certain weighted operation to minimize noise and reflection. sharpen the peak of cross-correlated functions at the time delay, and finally use inverse Fourier transform to transform into the time domain for time-delay estimation. This method can provide relatively accurate time-delay estimation. In addition, the windowing method can be used to process received target signal in order to prevent the loss of information of the target signal. Common window functions include Hamming and Hanning windows.

Assuming the signals received by two array elements are $x_1(t)$ and $x_2(t)$, according to the relationship of cross-correlated functions and cross-power spectrum, the expression is as follows:

$$R_{12}(\tau) = \int_0^{\pi} G_{x,x}(\omega) e^{-j\omega t} d\omega \tag{6}$$

where $G_{x_1x_2}(\omega) = E\{X_1(\omega)X_2^*(\omega)\}$ is the cross-power spectrum of two signals $x_1(t)$ and $x_2(t)$ received by two elements, $X_1(\omega)$ is the power spectrum sequence of signal sequence $x_1(t)$ after Fourier transformation from time domain to frequency domain, and $X_2^*(\omega)$ is the conjugate of signal $x_2(t)$ after transformation to frequency domain. Based on the principles of the GCC method, expression for GCC can be obtained as

$$R_{x_1x_2}(\tau) = \int_0^{\pi} \psi_{12}(\omega) G_{x_1x_2}(\omega) e^{-j\omega t} d\omega = \int_0^{\pi} \phi_{12}(\omega) G_{12}(\omega) e^{-j\omega t} d\omega, \quad (7)$$

where $\psi_{12}(\omega)$ is the weight function and $\phi_{12}(\omega) = \psi_{12}(\omega)G_{x_1x_2}(\omega)$ is the generalized cross-power spectrum. The time delay $\tau = argmax$ $R_{x,x}(\tau)$ can be obtained after inverse Fourier transform of the cross-power spectrum, and the peak position of $R_{x_1x_2}(\tau)$ is the time difference of the signal received by these two elements.

As shown in Eq. (7), different weighting functions may result in different time-delay estimation methods that vary considerably in accuracy and computation level. Thus, choosing an appropriate weighting function is a highly important step. The choice of weighting function is usually based on the practical application to obtain accurate time delay. Based on the infrasound signals

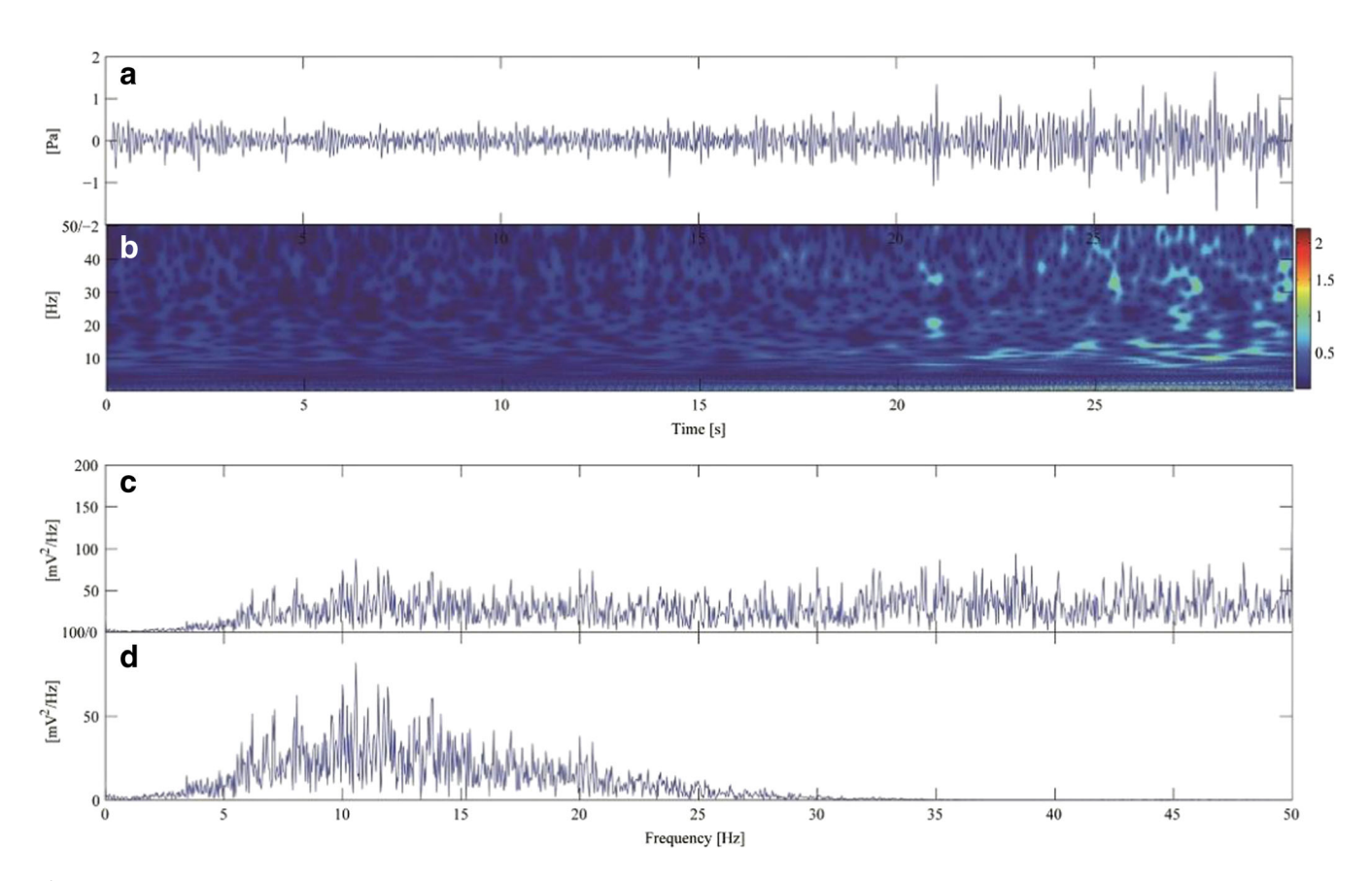


Fig. 10 A section of debris flow infrasonic signals received by device C during event 1. a Time series of original signals. b Time frequency spectrum of original signals. c Power spectra of original signals. d Power spectra of signals through low-pass filtered signals

collected from field observations and simulation tests of debris flows (include viscous and diluted), we compared different weighting methods (ROTH, SCOT, PHAT, and ML) under different signal-to-noise ratios (e.g., 20, 10, 0, and - 5 dB) and concluded that the time-delay estimation method based on the PHAT weighted cross-power spectrum phase (CSP) has the highest accuracy (Liu 2015). Therefore, the CSP algorithm was used in this study to estimate the time delay of infrasound signal from debris flow.

Set-up of real-time localization system

The monitoring array deployed in this study used three infrasound monitoring devices for debris flow to construct an irregular triangle array according to monitored topography and other factors that could affect the propagation of infrasound. The coordinates of each element are $A(X_A, Y_A)$, $B(X_B, Y_B)$, and $C(X_C, Y_C)$ (Xian 80 coordinate system). Based on the coordinates of each element, the distance between elements can be obtained, set as AB = a, BC = b, and AC = c. This triangle is then translated such that element B is set at origin, with coordinates of (0, 0), element C at the positive xaxis, with coordinates of (b, o), element A in the first quadrant. Assuming P(x, y) is the position of the target acoustic source, as shown in Fig. 5, the coordinates of $A(x_A, y_A)$ can be calculated using the following equation set:

$$\begin{cases} x_A^2 + y_A^2 = a^2 \\ (x_A - b)^2 + y_A^2 = c^2 \end{cases}$$
 (8)

Solving this equation set gives x_A and y_A as

$$\begin{cases} x_A = \frac{a^2 + b^2 - c^2}{2b} \\ y_A = \frac{1}{2b} \sqrt{(a+b+c)(a+b-c)(a-b+c)(b-a+c)} \end{cases}$$

It is well known that after a series of translation of a triangle on 2D surface, only the coordinates of vertices change, while the lengths of sides and the distances between point P and each vertex remain the same. Therefore, the following relationship is satisfied after the translation of Δ *ABC*:

$$\begin{cases}
PA-PB = v^* \tau_{AB} \\
PB-PC = v^* \tau_{BC} \\
PA-PC = v^* \tau_{AC} \\
\tau_{AB} + \tau_{BC} = \tau_{AC}
\end{cases}$$
(10)

where v is the speed of infrasound in air at room temperature (340 m/s in this study), τ_{AB} , τ_{BC} , and τ_{AC} are the time difference for signal to arrive at points A, B, and C from target acoustic source P, respectively.

Assume PC = z, $v^* \tau_{BC} = m$, $v^* \tau_{AC} = n$, then PB = z + m; PA = z + n, satisfying the following equation set:

$$\begin{cases} (x-b)^2 + y^2 = z^2 \\ x^2 + y^2 = (z+m)^2 \\ (x-x_A)^2 + (y-y_A)^2 = (z+n)^2 \end{cases}$$
(11)

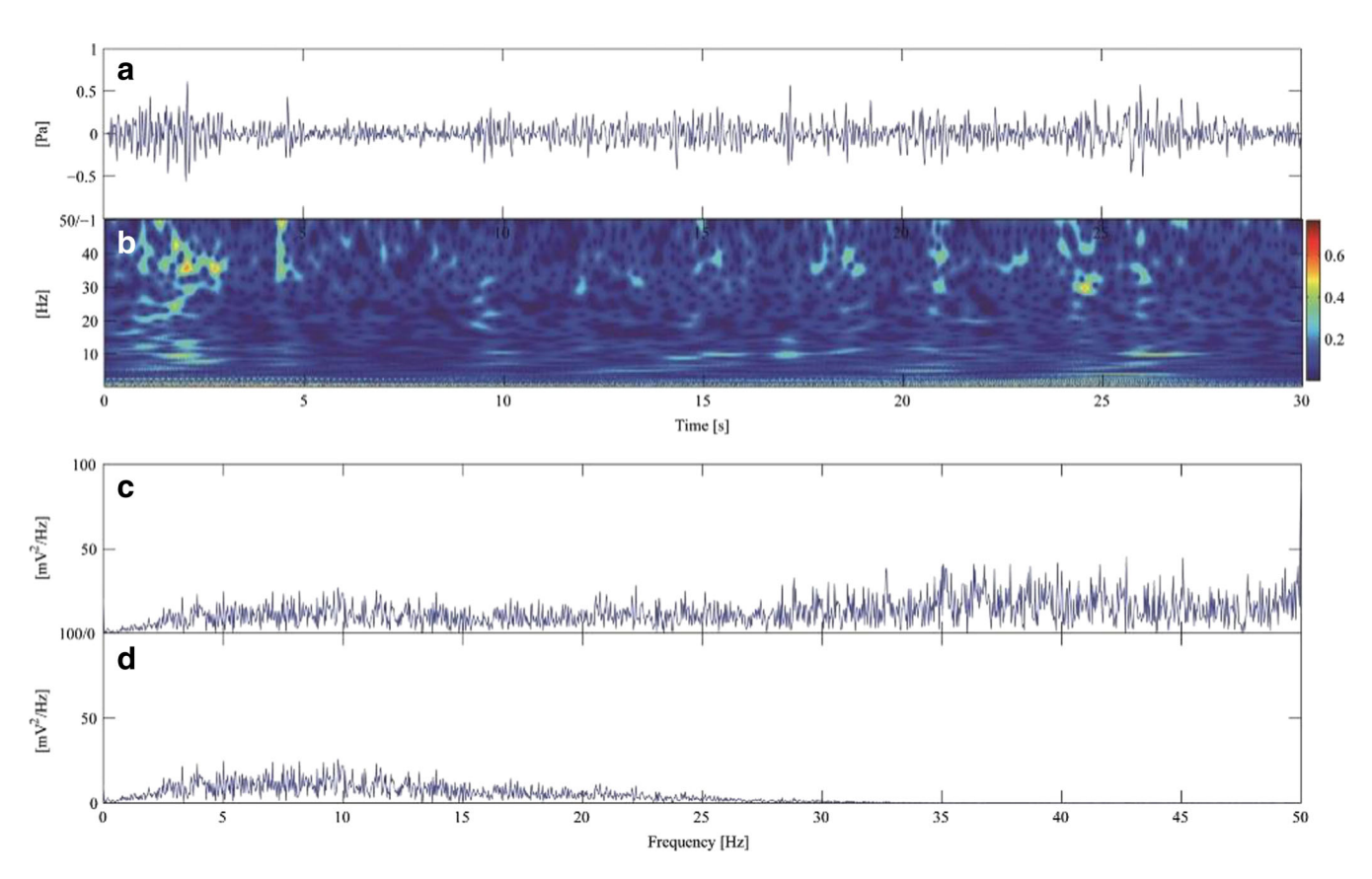


Fig. 11 A section of debris flow infrasonic signals received by device B during event 2. a Time series of original signals. b Time frequency spectrum of original signals. c Power spectra of original signals. d Power spectra of signals through low-pass filtered signals

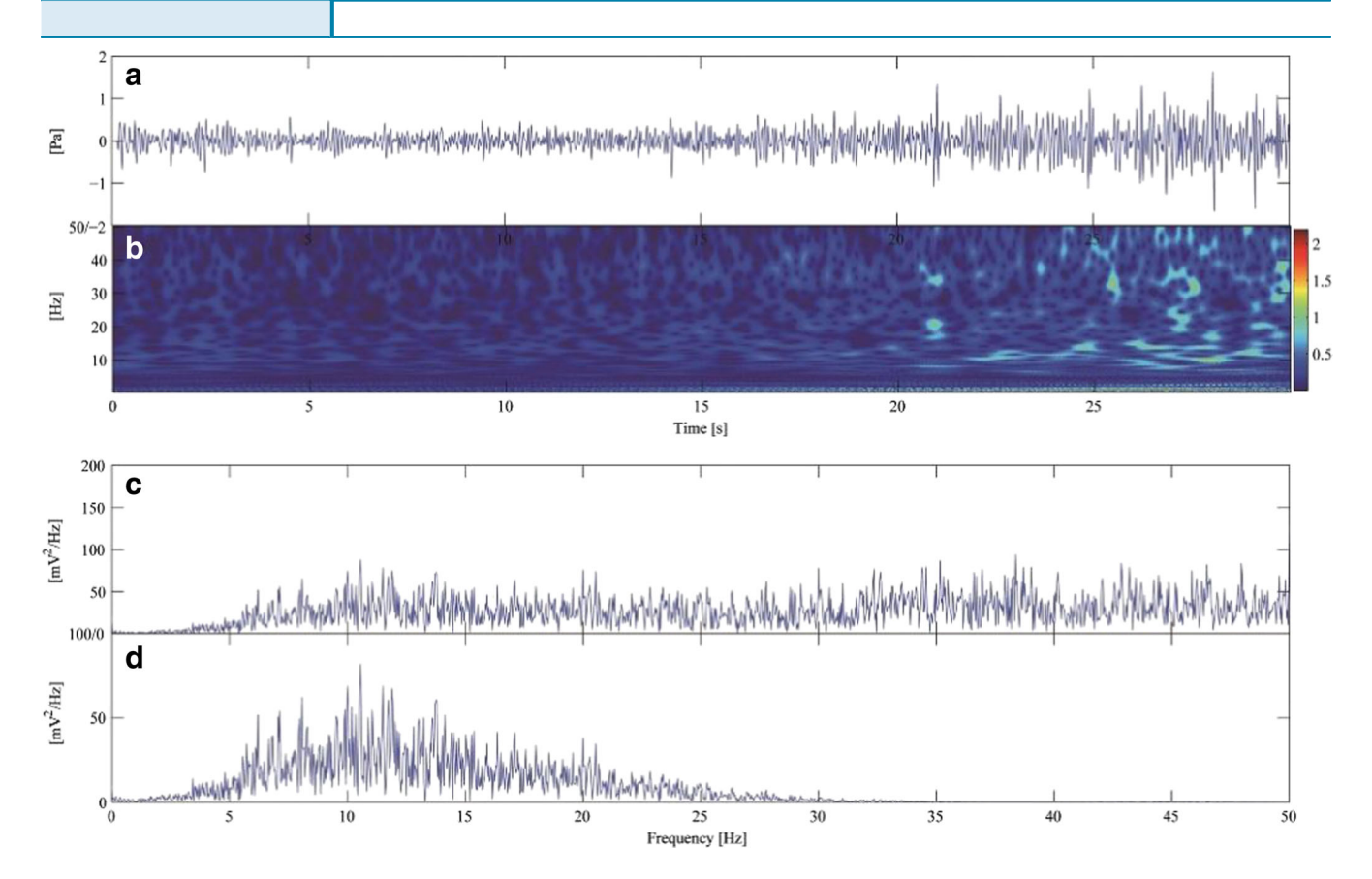


Fig. 12 A section of debris flow infrasonic signals received by device C during event 2. a Time series of original signals. b Time frequency spectrum of original signals. c Power spectra of original signals. d Power spectra of signals through low-pass filtered signals

Solving this equation set gives the coordinate of P in the Xian 80 coordinate system. Converting the solved coordinates into latitude and longitude in the WGS84 coordinate system allows us to obtain the position of the infrasound source:

$$\begin{cases} x = \frac{k_1 \cdot n - h_1 \cdot m}{h_2 \cdot k_1 - h_1 \cdot k_2} \\ y = \frac{k_2 \cdot n - h_2 \cdot m}{h_1 \cdot k_2 - h_2 \cdot k_1} \\ k_1 = X_B - X_C \\ k_2 = Y_B - Y_C \\ h_1 = X_A - X_C \\ h_2 = Y_A - Y_C \end{cases}$$
(12)

The time difference for a target signal to arrive at different elements in the array can be estimated at a certain interval (such as 30 s) by the aforementioned time-delay estimation method. Based on the derived equation for the location of the infrasound source, a complete location system for the position of the infrasound source can be established with the help of a GIS platform, fulfilling the visualized localization and real-time tracking of the debris flow movement. This system has high computational efficiency, ease of operation, high accuracy of localization, and strong real-time capability.

Test on real-time localization and tracking system of debris flow

Simulation test on the system

The infrasound generated by drumming and blasting was set as the target signal to verify the aforementioned time-delay estimation

method and acoustic source localization system. In this paper, two sets of drumming and blasting tests are selected to be elaborated in detail. Based on the range of dominant frequency of infrasound signals from drumming and blasting (around 4.3-17.2 and 0.4-16.7 Hz), bandpass filtering was conducted to amplify the effective signal-to-noise ratio of the infrasound signal and improve the accuracy of the time-delay estimation.

(1) Simulation test by drumming

The coordinates of three monitoring devices were A (103.131233° E, 26.248433° N), B (103.130902° E, 26.248927° N), and C (103.130647° E, 26.248088° N). The coordinates of the drum were P (103.131058° E, 26.248533° N). The distances between the acoustic source and the three devices were PA = 22.09 m, PB = 45.31 m, and PC = 63.76 m, respectively. Half-overlapping Hanning windowing was used to process the infrasound signal from the drumming. The aforementioned time-delay estimation method was used to analyze these two sets of test signals, and the maximum correlation coefficient (R) and time-delay (τ) between signals received by these three devices were obtained. The first set of tests yielded the following: $R_{AB} = 0.78$, $R_{BC} = 0.76$, $\tau_{AB} = -0.04$ s, $\tau_{BC} = -0.07$ s, thus $\tau_{AC} = \tau_{AB} + \tau_{BC} = -$ o.11 s. The second set of tests produced results as follows: $R_{AB} = 0.69$, $R_{BC} = 0.77$; $\tau_{AB} = -0.05$ s, $\tau_{BC} = -0.04$ s, thus $\tau_{AC} = \tau_{AB} + \tau_{BC} = -$ 0.09 s. Therefore, based on the first test of time-delay estimation, we derived the following: $PA - PB = \upsilon \times \tau_{AB} = -13.76$ m, $PB - PC = \upsilon \times \tau_{BC}$ = 24.08 m, and $PA - PC = \upsilon \times \tau_{AC}$ = 37.84 m. The coordinate of position of acoustic source P_1 was (103.131008° E, 26.248571° N), which was within 6.9 m of the real drumming location. Based on the

time delay of the second set of tests, we derived that $PA - PB = v \times v$ $au_{AB} = -17.2$ m, $PB - PC = \upsilon \times \tau_{BC} = 13.76$ m, and $PA - PC = \upsilon \times \tau_{BC} = 13.76$ τ_{AC} = 30.96 m. The coordinate of position of the acoustic source P_2 was (103.130973° E, 26.248526° N), which was within 7.8 m of the real drumming location. The location results of the two sets of drumming tests are shown in Fig. 6.

Simulation test by blasting

The coordinates of three monitoring devices were A (103.131233° E, 26.248433° N), B (103.132830° E, 26.247801° N), and C (103.133238° E, 26.248159° N). The coordinates of the explosion were P (103.132983° E, 26.248013° N). The distances between the acoustic source and three devices were PA = 42.31 m, PB = 26.49 m, and PC = 30.53 m, respectively. Half-overlapping Hanning windowing was again used to process the infrasound signal from the blasting. The aforementioned time-delay estimation method was used to analyze these two sets of test signals, and the maximum correlation coefficient (R) and time delay (τ) between signals received by these three devices were obtained. The first set of tests yielded the following: $R_{AB} = 0.82$, $R_{BC} = 0.66$; $\tau_{AB} = 0.03 \text{ s}, \tau_{BC} = 0.01 \text{ s}, \text{ thus } \tau_{AC} = \tau_{AB} + \tau_{BC} = 0.04 \text{ s}.$ The second set of tests produced the following results: $R_{AB} = 0.78$, $R_{BC} = 0.81$; $\tau_{AB}=$ 0.04 s, $\tau_{BC}=$ 0 s, thus $\tau_{AC}=\tau_{AB}+\tau_{BC}=$ 0.04 s. Therefore, based on the first test of time-delay estimation, we derived that $PA - PB = v \times v$ τ_{AB} = 10.32 m, $PB - PC = \upsilon \times \tau_{BC}$ = 3.44 m and $PA - PC = \upsilon \times$ τ_{AC} = 13.76 m. The coordinates of the position of acoustic source P_1 was (103.132989° E, 26.248044° N), which was within 4.6 m from the

real blasting location. Based on the time delay of the second set of tests, we derived that $PA - PB = \upsilon \times \tau_{AB} = 13.76 \text{ m}$, $PB - PC = \upsilon \times \tau_{BC} = 0 \text{ m}$, and $PA - PC = v \times \tau_{AC} = 13.76$ m. The coordinate of position of the acoustic source P_2 was (103.132993° E, 26.248017° N), which was within 1.7 m from the real blasting location. The location results of the two sets of firework tests are shown in Fig. 7.

Based on the location of monitoring devices and the acoustic source, the differences of their distances can be derived as PA - PB = -23.22 m, PB - PC = -18.45 m, and PA - PC = -41.67 m. The accuracy of the adopted time-delay estimation method was evaluated by comparing the calculated and measured difference in the distance between monitoring devices and the acoustic source. The differences in the first set of drumming tests were 9.46, 5.63, and 3.83 m, the differences for the second set of drumming tests were 6.02, 4.69, and 10.71 m; the differences for the first set of blasting tests were 5.51, 0.6, and 1.98 m, and the differences for the second set of blasting test were 2.07, 4.04, and 1.98 m. Based on the comparison between calculated and actual coordinates of the acoustic source, the accuracy of the established location system for the acoustic source can be evaluated. The difference from the first set of drumming test was 6.9 m, the difference from the second set of drumming test was 7.8 m, the difference from the first set of blasting test was 4.6 m, and the difference from the second set of blasting test was 1.7 m. Because of the large signal-to-noise ratio in the environment of the blasting test, its accuracy on the time-delay estimation is relatively high. The location results from these two sets of tests show that the distance between calculated and actual locations of acoustic source are very similar, with a maximum error of 7.8 m. This location result shows

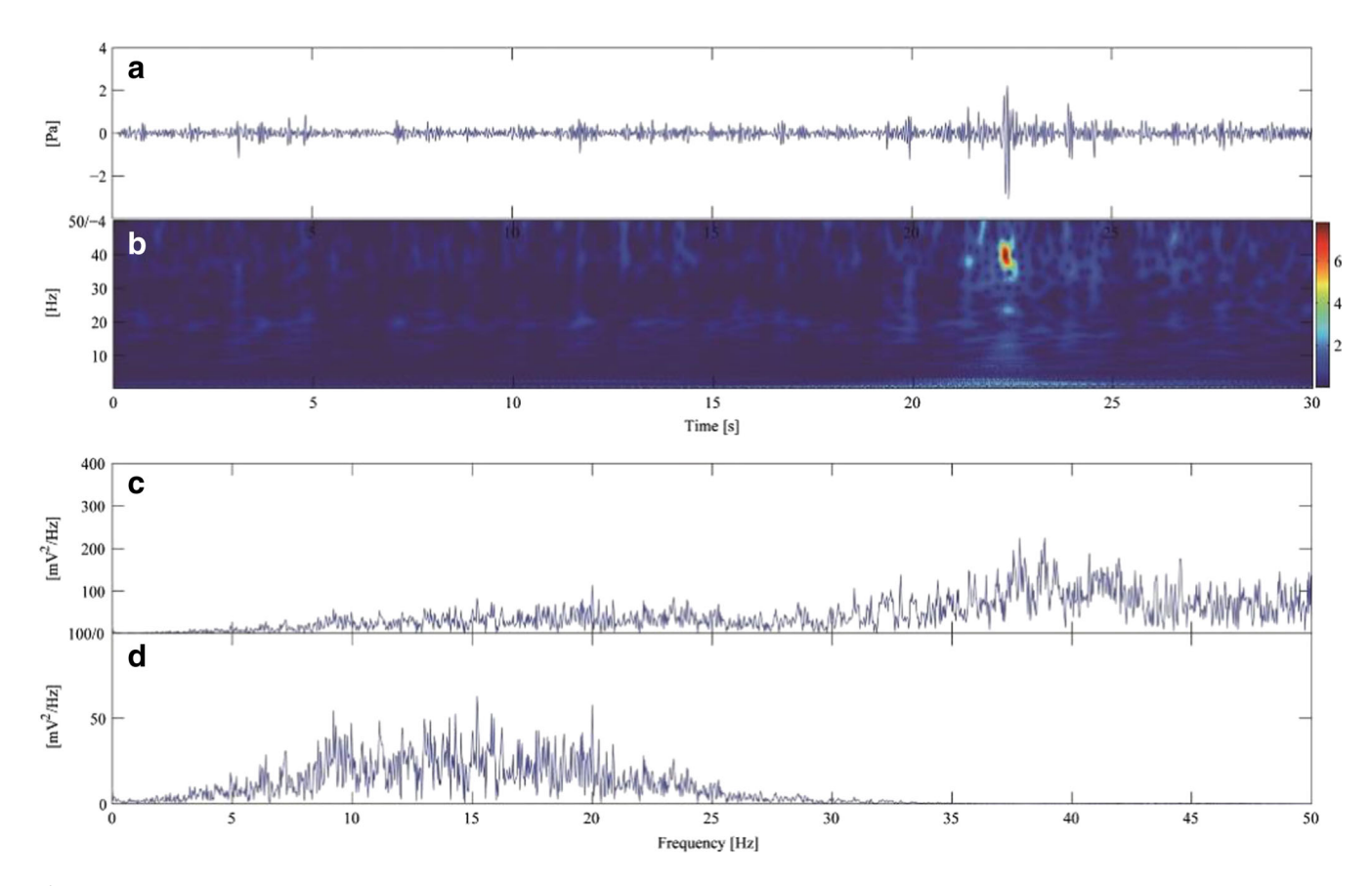


Fig. 13 A section of debris flow infrasonic signals received by device A during event 3. a Time series of original signals. b Time frequency spectrum of original signals. c Power spectra of original signals. d Power spectra of signals through low-pass filtered signals

that the time-delay estimation method and the acoustic source location system have high accuracy, sufficiently meeting the localization need of infrasound generated by debris flow.

Field test of the system at Jiangjia gully

The frequent debris flow in Jiangiia gully and the observation stations for debris flow at Dongchuan established by the Chinese Academy of Sciences provide very convenient conditions for the field test and result verification of the infrasound monitoring and localization system. Therefore, the system was deployed in Jiangjia gully to verify its effectiveness in monitoring debris flow. Based on the topography of Jiangjia gully and strength of the GPRS network, three devices were deployed on the two sides of the gully to constitute a monitoring array (Fig. 8). This deployment was selected to minimize the influence by human activity and receive the infrasonic signal generated by the debris flow very well.

Through the long-term site monitoring, we confirmed that four debris flow events occurred during July to August 2014 (event 1: July 28 15:12:21–15:55:01; event 2: August 4, 12:20:01–13:08:41; event 3: August 4, 18:21:21-18:53:31; and event 4: 20:52:51-23:46:31). Of these four events, events 1 and 2 were small-scale diluted debris flows, and infrasound signals with strong characteristics of debris flow were only received by devices B and C (the signal monitored by device A, which was located in the most downstream area, did not show characteristics of debris flow). Therefore, the position could not be located (number of elements that received target signal was less than 3). Figures 9, 10, 11, and 12 show the infrasound signals from debris flow received by devices B and C during events 1 and 2.

Event 3 was diluted debris flow that has a short duration but large scale. All three devices received infrasonic signals that had strong characteristics of debris flow. Event 4 was viscous debris flow, lasting several hours and was large in scale. All monitored signals from the three devices showed obvious characteristics of debris flow during event 4. Figures 13 and 14 show the infrasound signal from debris flow detected by device A during events 3 and 4 (Fig. 13: 18:40:11-18:40:41; Fig. 14: 22:56:31-22:57:01).

Localizations were regarded as effective when signals monitored by all three devices were in a good state (cross-correlation coefficient > 0.5); otherwise, the localization was considered to be false. Here, one effective localization during event 4 was taken as an example to explain the process of real-time location (time period: 22:56:41-22:57:01). The other localization processes in other time periods were similar.

Debris flow was initiated from the upstream provenance region and moved downstream. Device C was the first to receive the infrasound signal from the debris flow. Therefore, device C was set as the reference. The monitored signal detected by device C between 22:56:41 and 22:57:01 was determined as reference signal. The other two signals that were used for cross-correlation analysis were those monitored by devices A and B over the same period (Fig. 15). The Hanning window with frameshift of 500 sampling points and length of 1000 sampling points was used for the frame

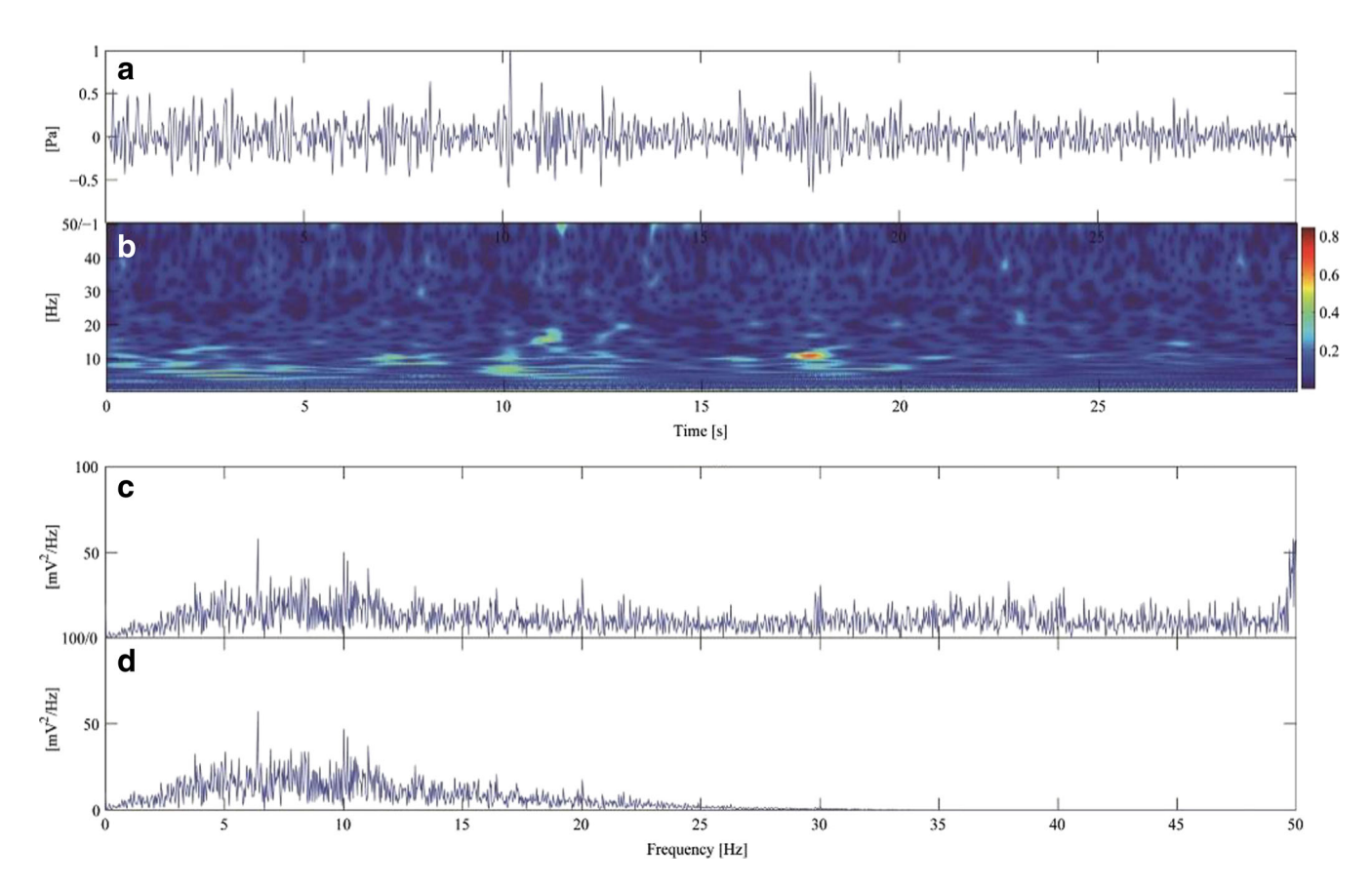


Fig. 14 A section of debris flow infrasonic signals received by device A during event 4. a Time series of original signals. b Time frequency spectrum of original signals. c Power spectra of original signals. d Power spectra of signals through low-pass filtered signals

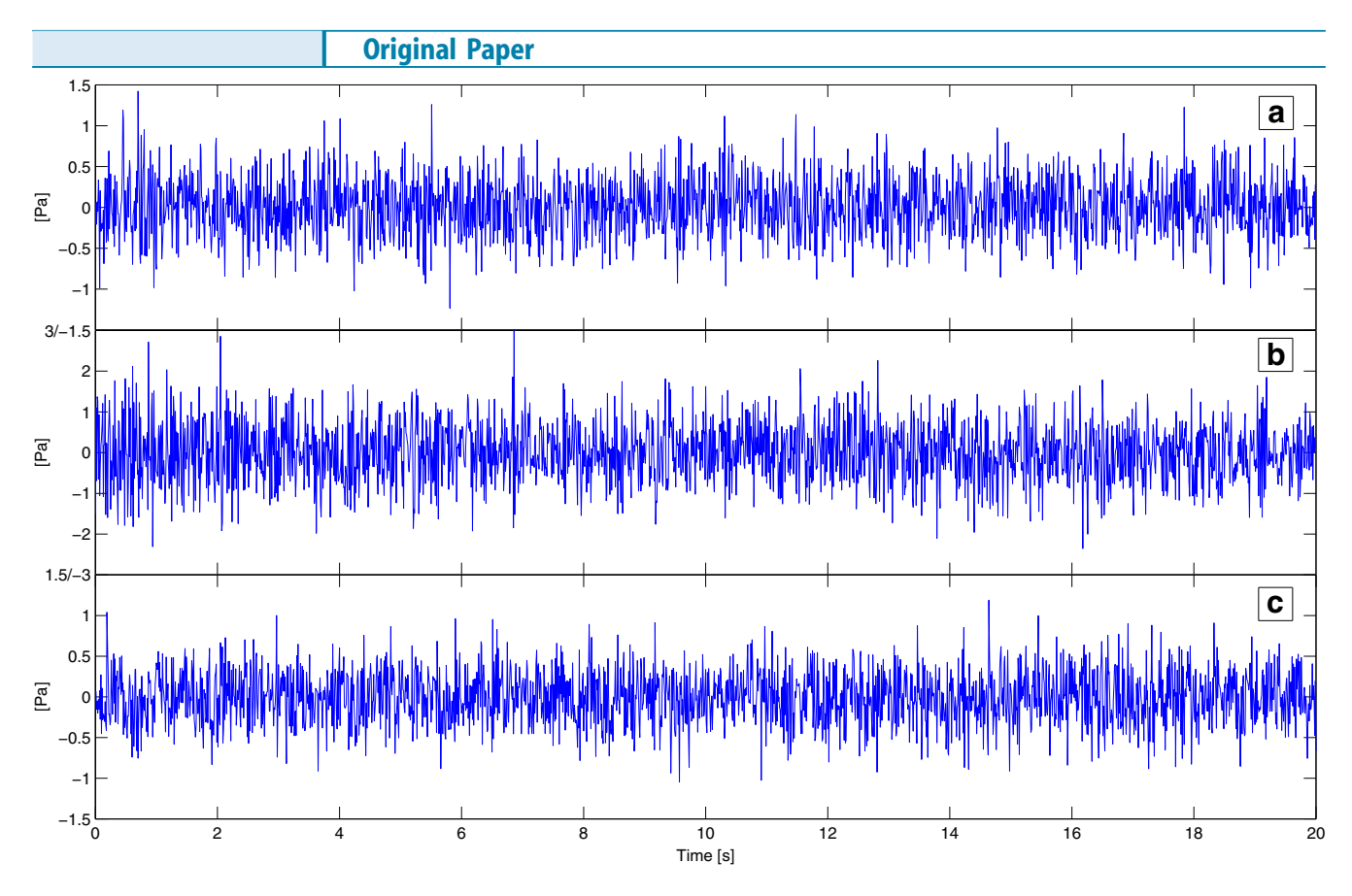


Fig. 15 Debris flow infrasonic signals received by devices A, B, and C in the period of 22:56:41–22:57:01

and window processing. Each segment had three frames of signal. Each frame in these three segments of signal was processed with 5-15 Hz bandpass filtering. Based on the determined time-delay estimation method, the correlation coefficient between the reference signal segment (device C) and the other two signal segments (A, B) were $R_{AC} = 0.76$ and $R_{BC} = 0.69$. The delay at the peak position was $Y_{AC} = -14$ and $Y_{BC} = -149$ (Fig. 16). According to the sampling frequency (100 Hz), the time differences were then calculated as τ_{AC} = - 0.14 s, τ_{BC} = - 1.49 s, and thus τ_{AB} = 1.35 s. Based on the obtained time difference between each pair of devices, the current longitude and latitude of debris flow was calculated by the acoustic source location system as (103.146044° E, 26.249945° N). In this way, the location of debris flow during this time period was determined.

By effective locating of debris flow movement in real time based on the aforementioned localization method, automatically removing false locations and drawing effective locations with the help of GIS visualization platform, we can achieve the real-time monitoring of movement of debris flow. Due to the debris flow gully was fixed, the real position in this gully can be corrected based on the shortest distance between the located position and the gully. Figures 17 and 18 show the corrected results of effective localization during the period of events 3 and 4 (Fig. 17: 18:25-18:50; Fig. 18: 21:00-22:10).

If the real location of debris flow in events 3 and 4 was known, the accuracy and error of this location system could be precisely analyzed. However, no camera was installed in the gully in this study; thus, the real-time movement of debris flow was not recorded. Therefore, based on the results of real-time localization

from the system and the trace of debris flow from field reconnaissance, the accuracy of the localization system was roughly evaluated. By analyzing all effective localization results, at least three surges occurred during event 3, and at least seven surges occurred during event 4. Further analysis showed that 71% of the location results were within 100 m from the trace of debris flow, about 82% location results were within 200 m from the trace of debris flow, about 89% location results were within 500 m from the trace of debris flow, and the other location results were all within 700 m from the trace of debris flow. The location results from these two events showed that this system can meet the need of visualized localization and real-time tracking of debris flow movement, providing more efficient monitoring and early alarm for debris flow.

Discussion and conclusion

Discussion

The current infrasound monitoring system for debris flow cannot locate and track debris flow in real time. To solve this problem, we deployed an array of infrasound sensors, and a location model for acoustic source was derived using the timedelay estimation method to estimate the time differences for the infrasound signal generated by debris flow to reach different elements. In addition, a visualized localization and tracking system was built to provide the optimal tracking of debris flow in real time. However, for the sake of further improving its accuracy on localization during application in the future, three problems need to be studied and addressed.

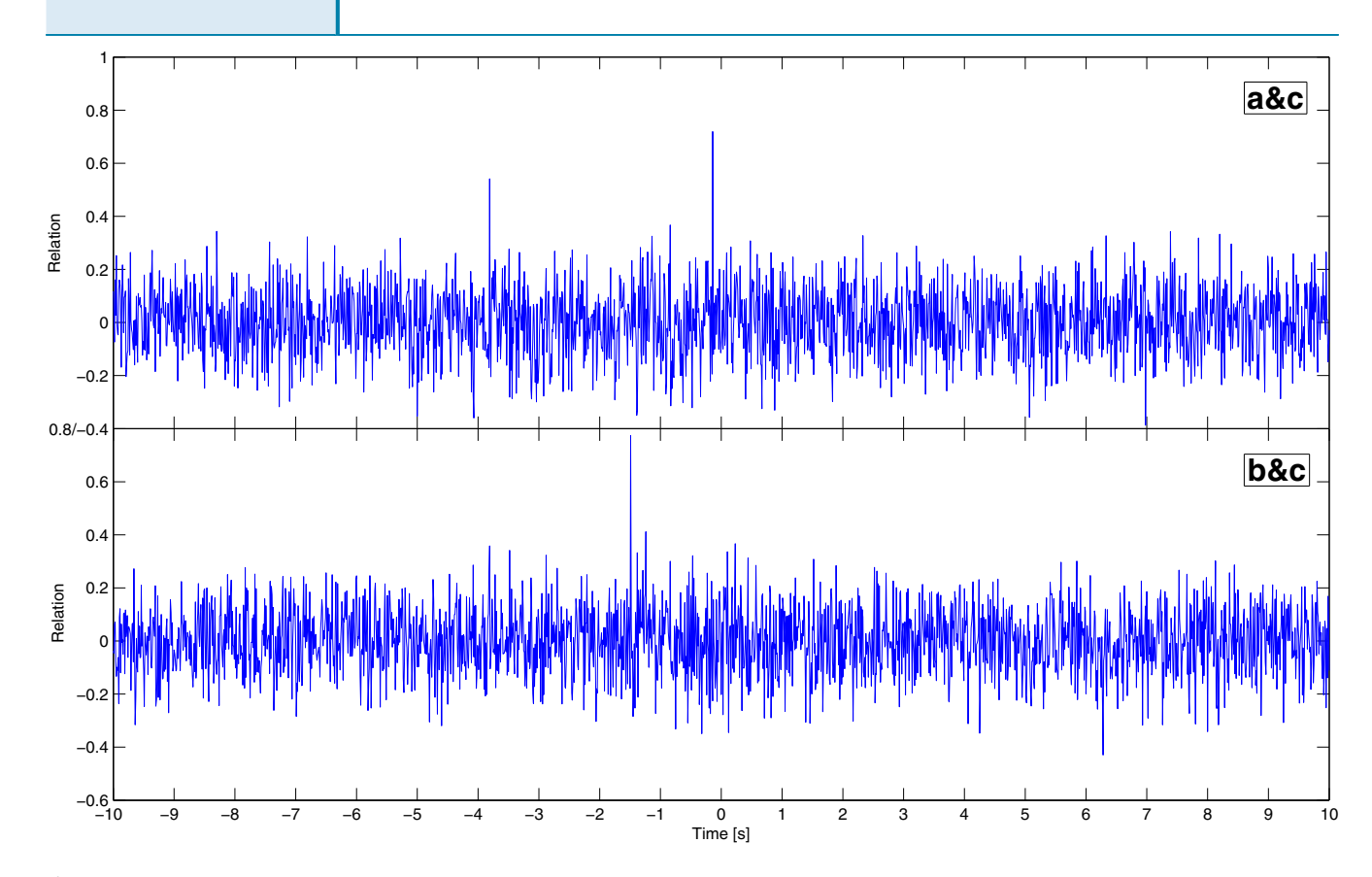


Fig. 16 Time delay values of debris flow infrasonic signals from devices A and C, B and C

- (1) This work adopted the simplest array structure. However, the topological structure, distance between elements, and number of elements can affect the accuracy of acoustic source localization. Therefore, it is necessary to add the number of elements, adjust the topological structure of the array and
- distance between elements, and develop a new localization model for the target acoustic source to improve the accuracy of location.
- The accuracy of the time difference of arrival also affects the accuracy of acoustic source localization. The key factors that

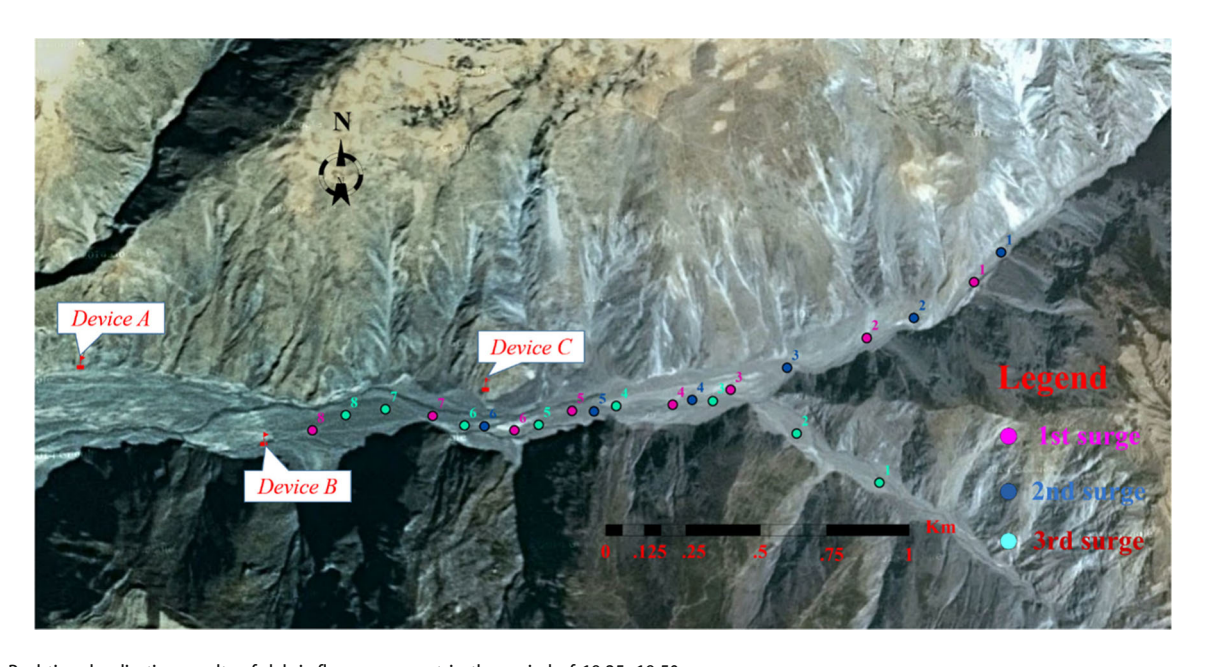


Fig. 17 Real-time localization results of debris flow movement in the period of 18:25-18:50

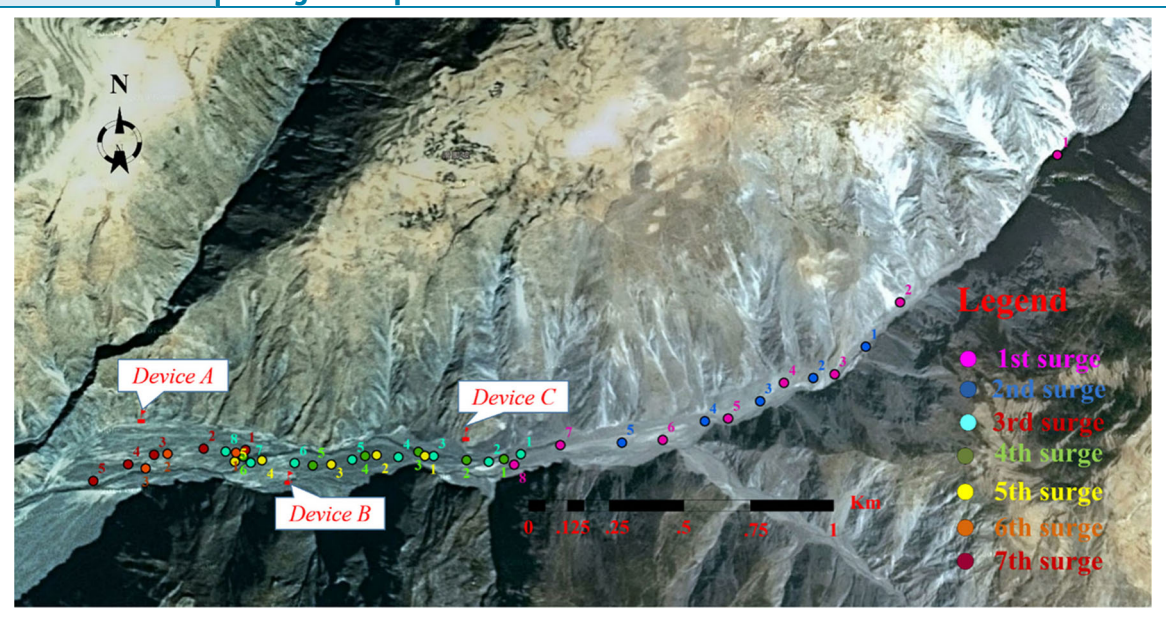


Fig. 18 Real-time localization results of debris flow movement in the period of 21:00-22:10

affect the time difference of arrival are the signal-to-noise ratio and time-delay estimation method. Therefore, more appropriate noise reduction measures should be taken in array deployment to increase the signal-to-noise ratio of infrasound. In addition, under the precondition of satisfying good real-time capability, the time-delay estimation method needs to be further improved to achieve better accuracy of time-delay estimation.

- (3) The monitoring array was deployed downstream of the Jiangjia gully, with little angle of elevation to the upstream monitoring area (< 15°), so the height of the target source has less influence on the positioning results. In addition, to reduce the computational complexity to meet the demand of real-time positioning, the impact of the height factor on positioning results was not considered in this study. In the subsequent research, if there is a large angle of elevation, it is necessary to improve the positioning model algorithm to achieve higher positioning accuracy under the precondition of satisfying good real-time capability.
- (4) The simulation test and field test of debris flow adopted the same method, but differed substantially in terms of location accuracy: the location error in simulation test was about 8 m, while that in field test was hundreds of meters. This was mainly due to the low sensitivity of the sensor. In the simulation test, the distance between each element was short, and the disturbance from noise was small, which causes a high signal-to-noise ratio. In the field test, however, the distance between each element was long, and environment was complex, which caused a low signal-to-noise ratio. Therefore, in order to track the real-time location of debris flow movement with higher accuracy, it is necessary to use a highly accurate infrasound sensor, and combine this with the new acoustic source localization model, noise reduction measures, and timedelay estimation method developed in response to (1) and (2).

Conclusion

In this study, we adopted a processing and analysis method with a combined SCM and upper computer. We fully utilized the strong data analyzing capability of upper computer and broke through the limit of single mode of integration processing by SCM, acceptably meeting the real-time requirement. Based on the geometric structure of monitoring array for infrasound and determined time-delay estimation method, a visualized localization and tracking system for debris flow monitoring based on infrasound was established in combination with a GIS platform, achieving more efficient infrasound monitoring for debris flow. The system was validated through simulation tests and a long-term field test at Jiangjia gully. Based on the results from the simulated test and practical applications, the following conclusions were drawn:

- This system has strong applicability for real-time tracking of debris flow. The only requirements to track and locate the movement of debris flow are the appropriate deployment of monitoring array based on the topology of monitored region, derivation of an acoustic source location model that is suitable for the array based on the time difference of arrival, and imbedding the location model into the system.
- The system has high accuracy in localization. The simulation test and field test both showed that this system has good visualized localization and tracking capability. Debris flow disaster prevention and reduction can be made based on the tracking results.
- This system has a strong real-time capability. The system (3) responded within 20-40 s after the infrasound signals from debris flow were received by each element. If the outside interference is small, localization can be achieved within only 20 s, whereas if the outside interference is strong, a longer time is needed to achieve effective localization.

Funding information

This research is supported by the Project (No. KYTZ201616) supported by the Scientific Research Foundation of CUIT and the National Natural Science Foundation of China (No. 41501114) and the College students' Innovative Entrepreneurial Training Plan (No. 201610621002) and the Science and Technology Service Network Initiative (No. KFJ-SW-STS-180).

References

- Bass HE, Bauer HJ, Evans LB (1972) Atmospheric absorption of sound: analytical expressions. J Acoust Soc Am 52(3B):821-825
- Cansi Y (1995) An automatic seismic event processing for detection and location: the PMCC method. Geophys Res Lett 22(9):1021-1024
- Chou HT, Cheung YL, Zhang SC (2007) Calibration of infrasound monitoring system and acoustic characteristics of debris-flow movement by field studies. The Fourth International Conference on Debeis-Flow Hazards Mitigation: Mechanics, Prediction, and Assessment. Chengdu, China, pp 571-580
- Chou HT, Chang YL, Zhang SC (2013) Acoustic signals and geophone response of rainfallinduced debris flows. J Chin Inst Eng 36(3):335-347. https://doi.org/10.1080/ 02533839.2012.730269
- Cook RK (1962) Strange sounds in the atmosphere. Part I. Sound Its Uses and Control 1(2):12-16. https://doi.org/10.1121/1.2369552
- Groot-Hedlin CDD, Hedlin MAH (2014) Infrasound detection of the Chelyabinsk meteor at the USArray. Earth Planet Sci Lett 402:337-345
- Hübl J, Zhang SC, Kogelnig A (2008) Infrasound measurements of debris flow. In: WIT Trans Eng Sci, vol 60, pp 3-12. https://doi.org/10.2495/DEB080011
- Johnson JB (2003) Generation and propagation of infrasonic airwaves from volcanic explosions, J Volcanol Geotherm Res 121(1):1-14
- Kogelnig A, Hübl J, Suriñach E, McArdell BW (2011) A study of infrasonic signals of debris flow. Italian Journal of Engineering Geology and Environment - Book, Proceedings of 5th international conference on debris-flow hazards: mitigation, mechanics, prediction and assessment. Padua, Italy, 563-572. https://doi.org/10.4408/IJEGE. 2011-
- Kogelnig A, Hübl J, Suriñach E, Vilajosana I, Mcardell BW (2014) Infrasound produced by debris flow: propagation and frequency content evolution. Nat Hazards 70(3):1713-1733. https://doi.org/10.1007/s11069-011-9741-8
- Jiang D 2002 A study of the direction of infrasonic origin on earthquake forecast. Thesis for Degree of Doctor of Beijing University of Technology. (In Chinese)
- Li CA, Hu YW, Wang LW (2012) Infrasound monitoring and early warning of debris flow along montanic railway line. Tech Acoust 31(4):351-356 (In Chinese)
- Li J, Wu R (1998) An efficient algorithm for time delay estimation. IEEE Trans Signal Process 46(8):2231-2235
- Liu DL, Leng XP, Wei FQ, Zhang SJ, Hong Y (2015) Monitoring and recognition of debris flow infrasonic signals. J Mt Sci 12(4):797-815
- Liu DL 2015 Debris flow positioning and real-time monitoring based on infrasound monitoring. Thesis for Degree of Doctor of University of Chinese Academy of Sciences. (In Chinese)
- Liu XL 2013 Study on infrasound source location and application based on microphone array. Thesis for Degree of Master of Taiyuan University of Science and Technology.
- Pichon AL, Herry P, Mialle P, Vergoz J, Brachet N, Garcés M, Drob D, Ceranna L (2005) Infrasound associated with 2004-2005 large Sumatra earthquakes and tsunami. Geophys Res Lett 32(19):L19802. https://doi.org/10.1029/2005GL023893
- Lu J, Yang Y (2012) Study on localization of infrasound waves radiated by natural events. J Acoust Soc Am 131(4):3351. https://doi.org/10.1121/1.4708560
- Lv J, Guo Q, Feng HN, Teng PX, Yang YC (2012) Anomalous infrasonic waves before a small earthquake in Beijing. Chin J Geophys 55(10):3379-3385 (In Chinese)
- Matoza RS, Hedlin MAH, Garcés MA (2007) An infrasound array study of Mount St. Helens. J Volcanol Geotherm Res 160(3):249-262. https://doi.org/10.1016/ j.jvolgeores.2006.10.006
- Matoza RS, Garcés MA, Chouet BA, D'Auria L, Hedlin MAH, Groot-Hedlin CD, Waite GP (2009) The source of infrasound associated with long period events at Mount St. Helens. J Geophys Res Solid Earth 114(B4). https://doi.org/10.1029/2008JB0061282

- Ma C, Wang YJ, Cui D, Wang YQ, Li YP (2016) Variation in initiation condition of debris flows in the mountain regions surrounding Beijing. Geomorphology 273:323-334
- Men CL, Gao WH, Feng HN, Yang YC (2011) Design of a wide-spread infrasound sensor array network system. Microcomput Appl 32(12):29-34. https://doi.org/10.3969/ i.issn.2095-347X.2011.12.006 (in Chinese)
- Murayama T, Honma M, Nogami M, Otsu T, Amano T (2006) Infrasound signals detected by the observation system in Isumi, Japan. J Acoust Soc Am 120(5):3032. https:// doi.org/10.1121/1.4787158
- Pilger C, Bittner M (2009) Infrasound from tropospheric sources: impact on mesopause temperature? J Atmos Sol Terr Phys 71(8):816-822
- Kang ZC (1993) Debris flow kinetic characteristics under natural conditions. J Hydrodyn 4:104-111
- Remillieux MC, Corcoran JM, Haac TR, Burdisso RA, Svensson UP (2012) Experimental and numerical study on the propagation of impulsive sound around buildings. Appl Acoust 73(10):1029-1044
- Ripepe M, De Angelis S, Lacanna G, Voight B (2010) Observation of infrasonic and gravity waves at Soufrière Hills Volcano, Montserrat. Geophys Res Lett 37(19):L00E14. https:// doi.org/10.1029/2010GL042557
- Wang Z, Li H, Shi KL, Zhao JW (2000) On improving time delay estimation precision of small size array. J Northwest Polytech Univ 18(1):142-146
- Wei XY, Guo Q, Men CL, Yang YC (2011) Design of widespread infrasound monitoring system. Audio Eng 35(5):47-49. https://doi.org/10.3969/j.issn.1002-8684.2011.05.013 (in Chinese)
- Zhang HX, Chen DY, Peng QQ, Shi L (2015) A revised TDOA wireless sensor network node location algorithm. Chin J Sensors Actuators 3:412-415
- Xu WJ, Guan HY, Wu XL (2013) Analysis of debris flow infrasound signal based on timefrequency analysis methods. Comput Modernization 1(4):36-39. https://doi.org/ 10.3969/j.issn.1006-2475.2013.04.009 (in Chinese)
- Yang YC, Ma CZ, Li XD, Tian J (2003) Algorithm study of fast and accurate time-delay estimation with fine interpolation of correlation peak. Acta Acust 28(2):159-166 (in
- Zhang SC, Yu NY (2008) Infrasonic Behavior of Debris Flow and Infrasonic Warning Device. In: SS Chernomorets (ed) Proceeding of International Conference: Debris Flow: Disasters, Risk, Forecast, Protection, Pyatigorsk, pp 22-29
- Zhang SC, Yu NY (2010) Early warning system to debris flow. J Mt Sci 28(3):379-384. https://doi.org/10.3969/j.issn.1008-2786.2010.03.017 (in Chinese)
- Zhang F, Yang QS, Xia YQ, Chen W (2013) Infrasound: a new frontier in monitoring earthquakes. Earth Sci Front 20(6):94-101
- Zhang GP, Xu J, Bi BG (2009) Relations of landslide and debris flow hazards to environmental factors. Chin J Appl Ecol 20(3):653-658
- Zhong DL, Zhang JS, Xie H, Cui P (2011) Techniques of debris flow alarm. J Mt Sci 29(2):234-242. https://doi.org/10.3969/j.issn.1008-2786.2011.02.013 (in Chinese)

D. Liu

College of Software Engineering, Chengdu University of Information Technology, Chengdu, 610225, China e-mail: ldl@cuit.edu.cn

X. Leng (🗷)

College of Information Science and Technology, Chengdu University of Technology, Chengdu, 610059, China e-mail: lengxiaopeng@cdut.cn

X. Leng · F. Wei · S. Zhang · Y. Hong

Institute of Mountain Hazards and Environment, Chinese Academy of Sciences, Chengdu, 610041, China